HEAT TRANSFER ENHANCEMENT FOR NATURAL CONVECTION FLOW OF WATER-BASED NANOFLUIDS IN A SQUARE ENCLOSURE

Ternik, P.[*] & Rudolf, R.[**],[***]

[*] Private Researcher, Bresterniška ulica 163, 2354 Bresternica, Slovenia

[**] University of Maribor, Faculty of Mechanical Engineering, Smetanova 17, 2000 Maribor, Slovenia

[***] Zlatarna Celje d.d., Kersnikova 19, 3000 Celje, Slovenia

E-Mail: pternik.researcher@gmail.com, rebeka.rudolf@uni-mb.si

Abstract

Numerical analysis is performed to examine the heat transfer enhancement of Au, Al_2O_3, Cu and TiO_2 water-based nanofluids. The analysis uses a two-dimensional enclosure under natural convection heat transfer conditions and has been carried out for the Rayleigh number range $10^3 \leq Ra \leq 10^5$, and for the nanoparticles' volume fraction range $0 \leq \varphi \leq 0,10$.

The governing equations were solved with the standard finite-volume method and the hydrodynamic and thermal fields were coupled together using the Boussinesq approximation. Highly accurate numerical results are presented in the form of average Nusselt number and heat transfer enhancement. The results indicate clearly that the average Nusselt number is an increasing function of both, Rayleigh number and volume fraction of nanoparticles. The results also indicate that heat transfer enhancement is possible using nanofluids in comparison to conventional fluids, resulting in the compactness of many industrial devices. However, low Rayleigh numbers show more enhancement compared to high Rayleigh numbers.

(Received in May 2011, accepted in October 2011. This paper was with the authors 2 months for 1 revision.)

Key Words: Natural Convection, Nanofluids, Square Cavity, Heat Transfer, Numerical Modelling

1. INTRODUCTION

The vast new world of nanotechnology provides fertile grounds for scientific advances and the development of novel devices as well as materials that affects the well-being of all. Among the various novelties scientists and engineers have introduced over the recent years are nanofluids which are extensively studied for their heat transfer properties, and could potentially enhance the efficiency of large-scale heat exchangers (used in chemical processing plants and HVAC systems) as well as smaller scale heat exchangers (used in the automotive and computer cooling sectors). In addition, other novel applications are being developed for mass transfer operations, for the harvesting of sunlight, and for imaging, sensing, transport and interactions in biological systems.

Thermal conductivity is an important parameter in determining the heat transfer characteristics of fluids and today more than ever, ultrahigh-performance heat transfer plays an important role in the development of energy-efficient heat transfer fluids which are required in many industries as well as commercial applications. However, the conventional heat transfer fluids (e.g. water, oil or ethylene glycol) are inherently poor heat transfer fluids and although various techniques are applied to enhance the heat transfer, the low heat transfer performance of these conventional fluids obstructs the performance enhancement and the compactness of heat exchangers. Since the thermal conductivity of solid materials are generally higher than those of fluids, suspended particles are expected to increase the thermal

conductivity and enhance heat transfer in fluid suspensions.

Nanofluid, a term coined by Choi [1] in 1995 is a new class of heat transfer fluids which is developed by suspending nanoparticles with the main goal to achieve the highest possible thermal properties at the smallest possible volume concentrations by uniform dispersion and stable suspension of nanoparticles in host fluids. Some nanoparticle materials that have been used in nanofluids are oxide ceramics (Al_2O_3, CuO), nitride ceramics (AlN, SiN), carbide ceramics (SiC, TiC), metals (Ag, Au, Cu, Fe), semiconductors (TiO_2), and single-, double-, or multi-walled carbon nanotubes (SWCNT, DWCNT, MWCNT).

Buoyancy induced flow and heat transfer is an important phenomenon used in various engineering systems. Some applications are solar thermal receivers, vapour absorption refrigerator units [2] and electronic cooling, selective laser melting process [3], steel quenching [4]. Studies on natural convection using nanofluids are very limited and they are mainly related with the differentially heated enclosures. Oztop and Abu-Nada [5] studied a two-dimensional natural convection of various nanofluids in partially heated rectangular cavities and reported that the type of nanofluid is a key factor for heat transfer enhancement. They obtained the best results with Cu nanoparticles. Hwang et al. [6] studied natural convection of a water based Al_2O_3 nanofluid in a rectangular cavity heated from below. They investigated the convective instability of the flow and heat transfer and reported that the natural convection of a nanofluid becomes more stable when the volume fraction of nanoparticles increases. Ho et al. [7] studied the effects on nanofluid heat transfer due to viscosity and thermal conductivity in a buoyant enclosure filled with alumina-water nanofluid. They demonstrated that usage of different models for viscosity and thermal conductivity has a major impact on heat transfer and flow characteristics. Heat transfer enhancement utilizing water-Cu and water-Al_2O_3 nanofluids in a trapezoidal enclosure was studied by numerical means in the work of Saleh et al. [8] with a focus on the effects of Grashof number, inclination angle of the sloping wall, volume fraction of nanoparticles on flow and temperature patterns as well as the heat transfer rate within the enclosure. They report that acute sloping wall and Cu nanoparticles with high concentration are effective to enhance the rate of heat transfer.

Effect of inclination angle on heat transfer enhancement under natural convection in square cavities has been studied by Oztop et al. [9] (Al_2O_3 and TiO_2 nanofluids), Abu-Nada and Oztop [10] (Cu nanofluids) and Ögüt [11] (Cu, Ag, CuO, Al_2O_3, and TiO_2 nanofluids). Their results show that effects of inclination angle on percentage of heat transfer enhancement become insignificant at low Rayleigh number but it decreases the enhancement of heat transfer with nanofluid and that the inclination angle is a good control parameter for both pure and nanofluid filled enclosures [8, 9]. It is also reported [8-10] that the average heat transfer increases significantly as particle volume fraction φ and Rayleigh number Ra increases.

The above review of the existing literature clearly indicates that the most widely studied nanoparticles are Al_2O_3, Cu and TiO_2. Framed in this general background, the aim of the present work is to undertake a comprehensive computational analysis on this topic, with the main scope to study the natural convection heat transfer characteristics in a square enclosure filled with water based Au nanofluids for the range of Rayleigh number $10^3 \leq Ra \leq 10^5$ and volume fraction $0 \leq \varphi \leq 0,10$. In addition, for the same range of Ra and φ we have numerically investigated the heat transfer characteristics for Al_2O_3, Cu and TiO_2 nanofluids allowing us to report the influence of nanoparticles type on the local and mean Nusselt number as well as heat on the transfer enhancement.

In the remaining of the present paper we present the governing equations and problem specification (Section 2). This is followed by the grid refinement, numerical accuracy assessment and validation study (Section 3) and the discussion of results in Section 4, prior to final remarks.

2. NUMERICAL MODELLING

The standard finite volume method is used to solve the coupled conservation equations of mass, momentum and energy. This method has been used successfully in a number of recent studies to simulate isothermal generalized Netwonian fluid flows [12, 13]. In the present framework, a second-order central differencing scheme is used for the diffusive terms and a third-order QUICK scheme for the convective terms. Coupling of the pressure and velocity is achieved using the well-known SIMPLE algorithm. The convergence criteria were set to 10^{-8} for all residuals.

2.1 Governing equations

For the present study steady-state flow of an incompressible water-based nanofluids is considered. It is assumed that both the fluid phase and nanoparticles are in thermal equilibrium. Except for the density the properties of nanoparticles and fluid are taken to be constant. Table I presents the thermo-physical properties of water and nanoparticles at the reference temperature. It is further assumed that the Boussinesq approximation is valid for the buoyancy force.

Table I: Thermo-physical properties of nanofluids.

	$\rho \, [kg / m^3]$	$c_p \, [J / kgK]$	$k \, [W / mK]$	$\beta \, [1 / K]$
Pure water	997,1	4179	0,613	$2,1 \times 10^{-4}$
Au	19320	128,8	314,4	$1,416 \times 10^{-7}$
Al_2O_3	3970	765	40	$8,5 \times 10^{-6}$
Cu	8933	385	400	$1,67 \times 10^{-5}$
TiO_2	4250	686,2	8,9538	$9,0 \times 10^{-6}$

The governing equations (mass, momentum and energy conservation) for a steady, laminar and incompressible flow are:

$$\frac{\partial v_i}{\partial x_i} = 0 \tag{1}$$

$$\rho_{nf} v_j \frac{\partial v_i}{\partial x_j} - \frac{\partial}{\partial x_j}\left(\eta_{nf} \frac{\partial v_i}{\partial x_j} \right) = -\frac{\partial p}{\partial x_i} + (\rho\beta)_{nf} g(T - T_C) + \frac{\partial}{\partial x_j}\left(\eta_{nf} \frac{\partial v_j}{\partial x_i} \right) \tag{2}$$

$$(\rho c_p)_{nf} v_j \frac{\partial T}{\partial x_j} = \frac{\partial}{\partial x_j}\left(k_{nf} \frac{\partial T}{\partial x_j} \right) \tag{3}$$

where the cold wall temperature T_C is taken to be the reference temperature for evaluating the buoyancy term $(\rho\beta)_{nf} g(T - T_C)$ in the momentum conservation equation.

Relationships between properties of nanofluid (*nf*) to those of pure fluid (*f*) and pure solid (*s*) are given with the following empirical models [9]:

- Density: $\rho_{nf} = (1-\varphi)\rho_f + \varphi\rho_s$
- Dynamic viscosity: $\eta_{nf} = \eta_f / (1-\varphi)^{2.5}$
- Thermal expansion: $(\rho\beta)_{nf} = (1-\varphi)(\rho\beta)_f + \varphi(\rho\beta)_s$

31

- Heat capacitance: $\left(\rho c_p\right)_{nf} = (1-\varphi)\left(\rho c_p\right)_f + \varphi\left(\rho c_p\right)_s$

- Thermal conductivity: $k_{nf} = k_f \dfrac{k_s + 2k_f - 2\varphi\left(k_f - k_s\right)}{k_s + 2k_f + \varphi\left(k_f - k_s\right)}$

2.2 Geometry and boundary conditions

The simulation domain and expected temperature distribution are shown schematically in Fig. 1. Two vertical walls of a square enclosure are kept at different constant temperatures ($T_H > T_C$), whereas the other boundaries are considered to be adiabatic in nature. Both velocity components (i.e. v_x and v_y) are identically zero on each boundary because of the no-slip condition and impenetrability of rigid boundaries. The temperatures for cold and hot vertical walls are specified ($T_{x=0} = T_H$, $T_{x=L} = T_C$). The adiabatic temperature boundary conditions for the horizontal insulated boundaries are given by $\partial T / \partial y = 0$ at $y = 0$ and $y = L$.
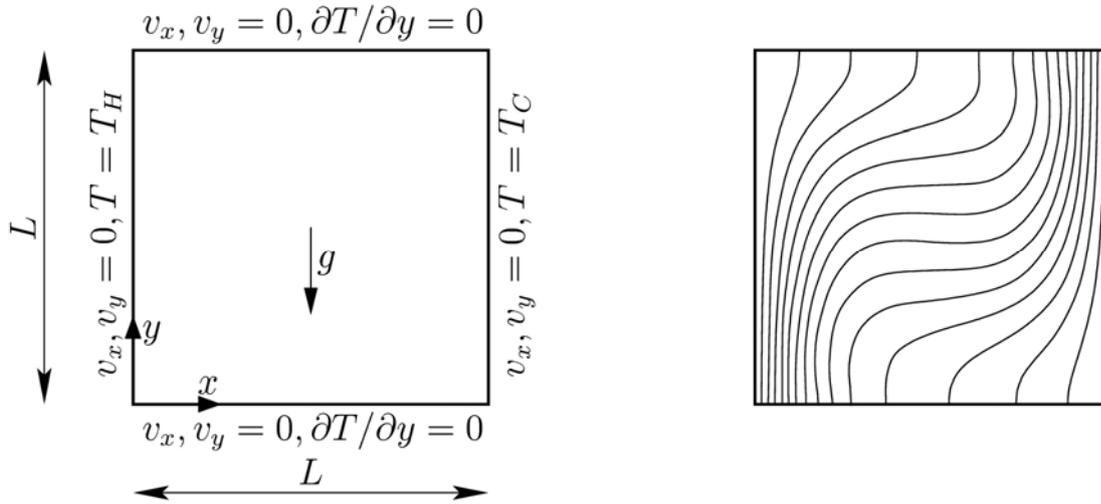

Figure 1: Simulation domain (left) and the expected temperature field (right).

In the present study, the heat transfer rates (along the hot vertical wall) in a square enclosure (of dimension L) with differentially heated sided walls filled with nanofluid are expressed in terms of the local and mean Nusselt number as follows:

$$Nu(y) = -\frac{k_{nf}}{k_f} \frac{\partial T(y)}{\partial x}\bigg|_{x=0} \frac{L}{T_{x=0} - T_C} \tag{4}$$

$$\overline{Nu} = \int_0^L Nu(y)\,dy\,/\,L \tag{5}$$

and compared with the heat transfer rate obtained in the case of pure water $\varphi = 0$ with the same nominal Rayleigh number. Here, the Rayleigh number Ra represents the ratio of the strengths of thermal transports due to buoyancy to thermal diffusion and is defined in the following manner:

$$Ra = \frac{\rho_{nf}\left(\rho c_p\right)_{nf} g\beta_{nf}\left(T_H - T_C\right)L^3}{\eta_{nf} k_{nf}} \tag{6}$$

3. GRID REFINEMENT, NUMERCAL ACCURACY AND VALIDATION

It should be one of the goals of each numerical analysis a comprehensive evaluation of CFD software used for particular application. Such an evaluation should ensure that different types of errors are identified, treated separately and reduced bellow an acceptable level.

In an ideal world this would mean that numerical solutions are provided for computational grids and time-steps, which are fine enough so that the numerical errors are small enough to be neglected. But on the other hand, this is not a trivial task and the separation (as well as study) of errors cannot always be achieved. Nevertheless, the worst strategy is to avoid this subject and to provide numerical simulations on a single computational grid, with single time-step and with other uncertainties in initial and boundary conditions not evaluated.

In the present work, the influence of computational grid refinement on numerical results was studied throughout the examination of spatial (grid) convergence. For this, the natural convection at $Ra = 10^5$ and $\varphi = 0,10$ was studied using four different uniform computational meshes; their main characteristics are given in Table II.

Table II: Computational mesh characteristics.

	N_x	N_y	$x^* = y^*$	N_{tot}
MI	40	40	0,025	1600
MII	80	80	0,0125	6400
MIII	160	160	0,00625	25600
MIV	320	320	0,003125	102400

The table includes the number of elements along the particular direction (N_x, N_y), normalized element size ($x^* = \Delta x / L$, $y^* = \Delta y / L$) and the total number of elements (N_{tot}) for particular mesh.

With each grid refinement the number of elements (i.e. control volumes) in particular direction is doubled and element size is halved. Such a procedure is useful for applying the Richardson's extrapolation technique which is a method for obtaining a higher-order estimate of the flow value (value at infinite grid) from a series of lower-order discrete values [14].

For a general primitive variable ϕ the grid-converged (i.e. extrapolated to the zero element size) value according to Richardson extrapolation is given as:

$$\phi_{ext} = \phi_{MIV} - \left(\phi_{MIII} - \phi_{MIV}\right)/\left(r^p - 1\right) \tag{7}$$

where ϕ_{MIV} is obtained on the finest grid and ϕ_{MIII} is the solution based on next level of coarse grid, $r = 2$ is ratio between the coarse to fine grid spacing and:

$$p = \ln\left[\left(\phi_{MII} - \phi_{MIII}\right)/\left(\phi_{MIII} - \phi_{MIV}\right)\right]/\ln 2 \tag{8}$$

is the observed order of convergence [15].

Table III: Effect of mesh refinement upon mean the Nusselt number ($Ra = 10^5$, $\varphi = 0,10$).

	MI	*MII*	*MIII*	*MIV*	$\overline{Nu}_{ext}$	*Error*
Au	5,4357	5,4816	5,4884	5,4892	5,4893	0,015
Al$_2$O$_3$	6,1226	6,1700	6,1780	6,1793	6,1795	0,024
Cu	6,0333	6,0792	6,0867	6,0879	6,0880	0,022
TiO$_2$	5,8948	5,9403	5,9481	5,9493	5,9495	0,024

The variation of the mean Nusselt number $\overline{Nu}$ with grid refinement is provided in tabulated form in Table III. The "percent" numerical error for the mean Nusselt number:

$$Error = \left| \left(\overline{Nu}_{MIII} - \overline{Nu}_{ext} \right) \middle/ \overline{Nu}_{ext} \right| \times 100\% \qquad (9)$$

as given in Table III is a quantification of the relative difference between the numerical predictions of $\overline{Nu}$ on *MIII* and the extrapolated values obtained from Richardson's extrapolation technique (denoted as $\overline{Nu}_{ext}$ in Table III). It can be seen that the differences with grid refinement are exceedingly small and the agreement between mesh *MIII* and extrapolated value is extremely good; the discretisation error for $\overline{Nu}$ is well below 0,03 %.

In addition to the aforementioned grid-dependency study, the present simulation results have also been compared against the well-known benchmark data of de Vahl Davis [16] and recent results of Turan et al. [17] for natural convection of air in a square cavity for the values of Rayleigh number $10^3 \leq Ra \leq 10^5$. The comparisons between the present numerical results (obtained with mesh *MIII*) with the benchmark values are extremely good and entirely consistent with our grid-dependency studies. The comparison is summarised in Table IV.

Table IV: Comparison of the present results with the benchmark values.

	$Ra = 10^3$		$Ra = 10^4$		$Ra = 10^5$	
	$\overline{Nu}$	Nu_{max}	$\overline{Nu}$	Nu_{max}	$\overline{Nu}$	Nu_{max}
Present study	1,118	1,506	2,245	3,532	4,521	7,724
de Vahl Davis [16]	1,118	1,506	2,243	3,528	4,519	7,717
Turan et al. [17]	1,118	1,506	2,245	3,531	4,520	7,717

All these results and comparison with existing numerical data from the literature gave sufficient confidence in the present numerical procedure allowing us to proceed with simulations for all nanofluids over the whole range of *Ra* and *φ*. Accounting for numerical accuracy and number of elements mesh *MIII* was found to be a good compromise and all results presented in continuation were obtained with this mesh.

4. RESULTS AND DISCUSSION

4.1 Mean Nusselt number

Variation of the mean Nusselt number (Eq. (5)) with solid volume fraction is shown in Figs. 2 and 3 which indicate that $\overline{Nu}$ increases with increasing *φ*. In the range $Ra \leq 10^4$, where the heat transfer is conduction dominated, the variation of $\overline{Nu}$ is linear for all water-based nanofluids studied herein (Fig. 2). The lowest heat transfer was obtained for TiO_2 nanofluid due to domination of conduction mode of heat transfer since TiO_2 has the lowest value of thermal conductivity compared to Au, Cu and Al_2O_3. Furthermore, due to similar value of thermal conductivity, Au and Cu nanofluids have almost identical variation of $\overline{Nu}$ with increasing *φ* in the range $Ra \leq 10^4$ (Fig. 2); the significant difference occurs at higher values of the Rayleigh number (Fig. 3).

As the Rayleigh number increases ($Ra \geq 10^4$), the variation of the mean Nusselt number becomes increasingly non-linear due to strengthened convective heat transport for Cu and especially Au nanofluids (Fig. 3), while increase in $\overline{Nu}$ with solid volume fraction remains linear for Al_2O_3 and TiO_2 nanofluids. Up to $φ \approx 0,05$, the highest heat transfer was obtained for Cu and Al_2O_3, followed by Au and TiO_2 nanofluids.

As the solid volume fraction further increases ($\varphi \geq 0{,}05$), the relative increase of heat transfer is smaller for Cu and especially Au nanofluids due to the high values of thermal diffusivity. The Au and Cu nanoparticles have high values of thermal diffusivity and, therefore, this reduces temperature gradients which will affect the performance of both, Au and Cu nanofluids.
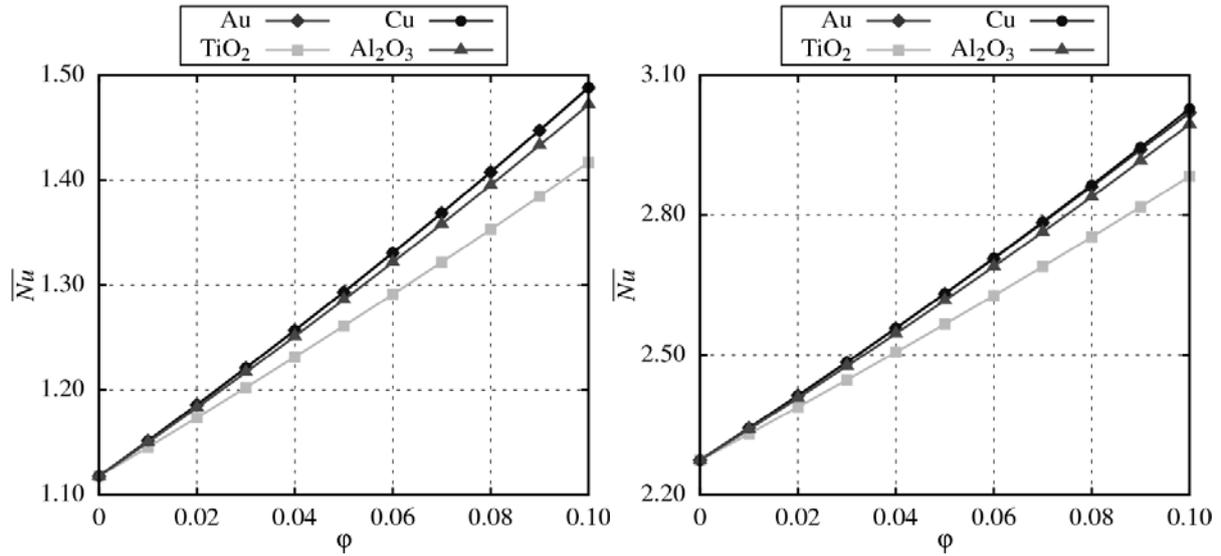
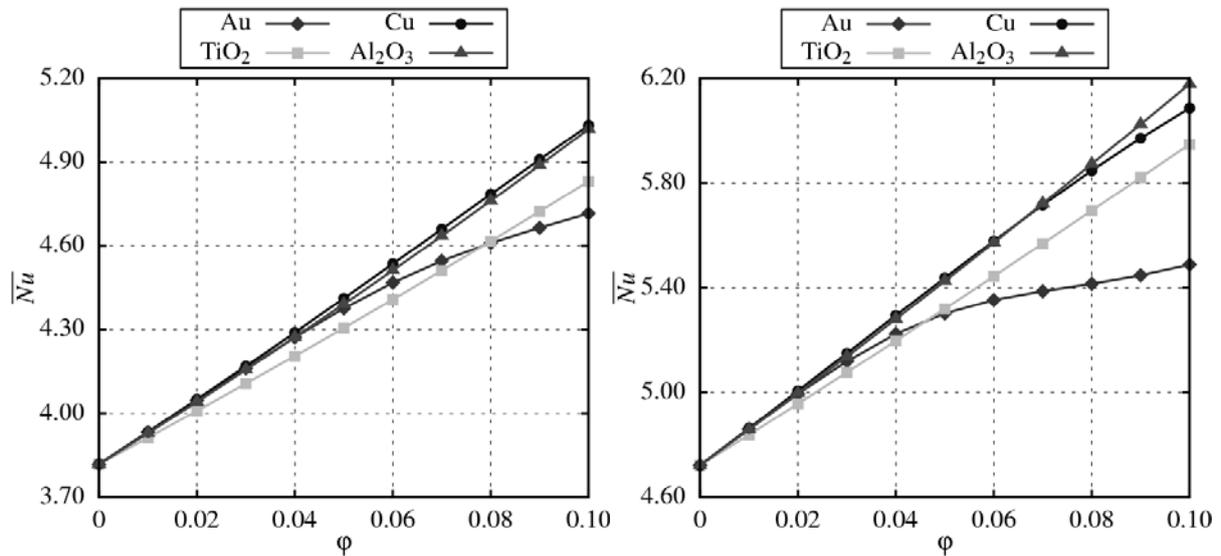Figure 2: Variation of $\overline{Nu}$ along the heated wall; $Ra = 10^3$ (left) and $Ra = 10^4$ (right).

Figure 3: Variation of $\overline{Nu}$ along the heated wall; $Ra = 5 \cdot 10^4$ (left) and $Ra = 10^5$ (right).

4.2 Heat transfer enhancement

The previous discussions indicate that generally heat transfer enhances (increase in mean Nusselt number) with addition of nanoparticle. To estimate the enhancement of heat transfer between the water-based nanofluid and the pure fluid ($\varphi = 0$) case, the enhancement is defined [10]:

$$E = \frac{\overline{Nu}(\varphi) - \overline{Nu}(\varphi = 0)}{\overline{Nu}(\varphi = 0)} \times 100\% \qquad (10)$$

Enhancement of heat transfer is plotted versus solid volume fraction for different values of Rayleigh number in Figs. 4 and 5. For the whole range of Rayleigh number values, the figures illustrate that enhancement of heat transfer increases for increasing solid volume fraction φ. It is an interesting observation that the heat transfer enhancement is an increasing linear function of volume fraction for Al_2O_3 and TiO_2 water-based nanofluids over the whole range of Ra, while Cu and Au nanofluids are characterized with non-linear increase in heat transfer enhancement at higher values of the Rayleigh number.
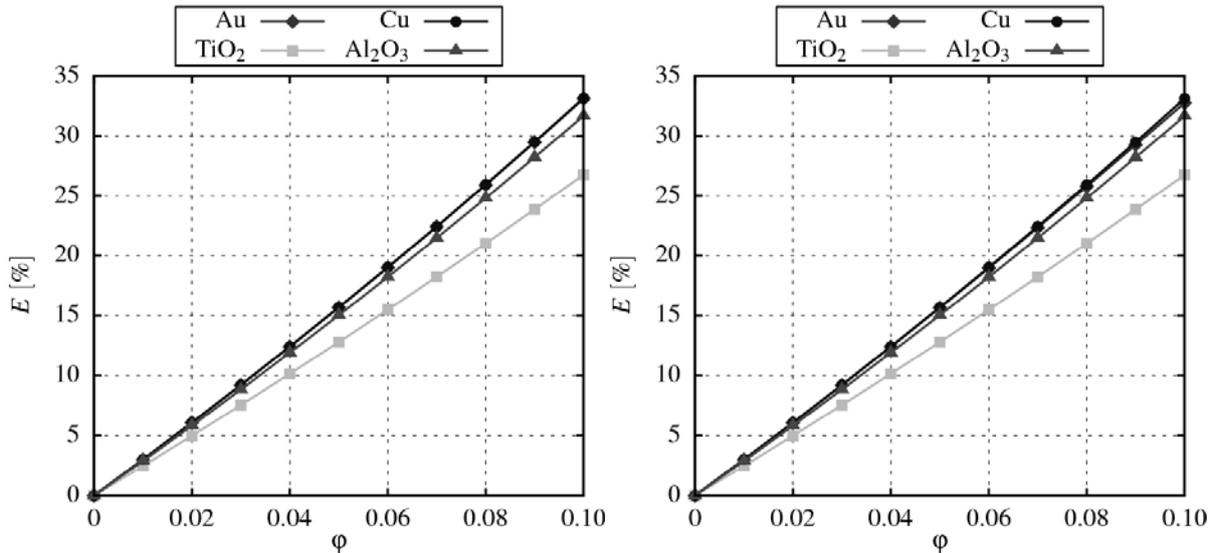
Figure 4: Heat transfer enhancement; $Ra = 10^3$ (left) and $Ra = 10^4$ (right).
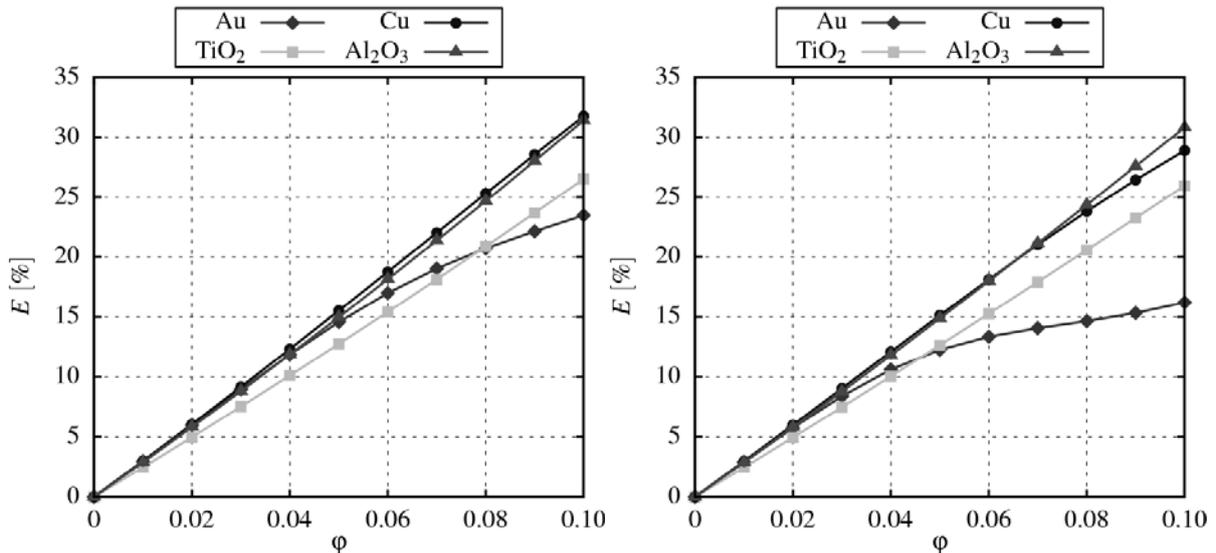

Figure 5: Heat transfer enhancement; $Ra = 5 \cdot 10^4$ (left) and $Ra = 10^5$ (right).

The relative increase of heat transfer in the convection dominated case ($Ra \geq 10^4$) is smaller than the increase in the conduction dominated case (heat transfer enhancement is greater for low Rayleigh numbers compared to high Rayleigh numbers) because the increased thermal conductivity does not play an important role in the convection dominated heat transfer (Figs. 6 and 7).

For example, for the Cu water-based nanofluid and $Ra = 10^3$ and $\varphi = 0{,}10$ the enhancement is approximately 33 % while for $Ra = 10^5$ and $\varphi = 0{,}10$ the enhancement is approximately 29 %. This observation can be explained by noting that at low Rayleigh

numbers the heat transfer is dominant by conduction and the viscous effects are less dominant. Therefore, the addition of high thermal conductivity nanoparticles increases the conduction and therefore makes the enhancement more effective. But on the other hand, at high values of Rayleigh number, the viscous effects become more effective and the influence of nanoparticles elucidates two opposing effects on the Nusselt number: a favourable effect driven by the presence of high thermal conductivity nanoparticles, and an undesirable effect promoted by the high level of viscosity experienced at the high volume fractions of nanoparticles. So, the high level of viscosity at high volume fractions of nanoparticles becomes more dominant, which reduces the heat transfer enhancement promoted by the high thermal conductivity.
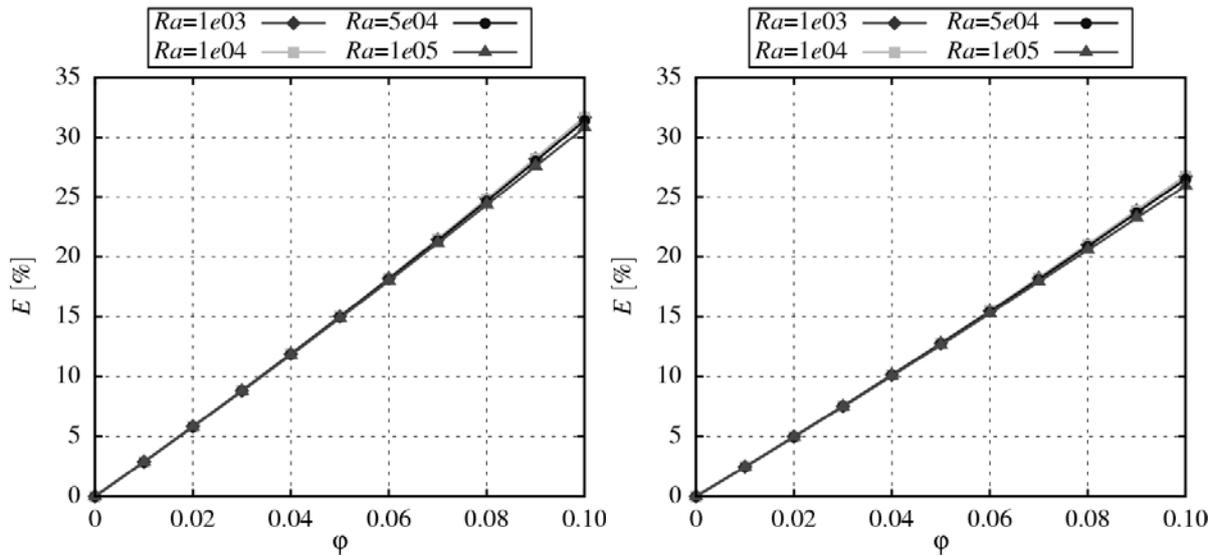

Figure 6: Heat transfer enhancement; Al_2O_3 (left) and TiO_2 (right) water-based nanofluid.
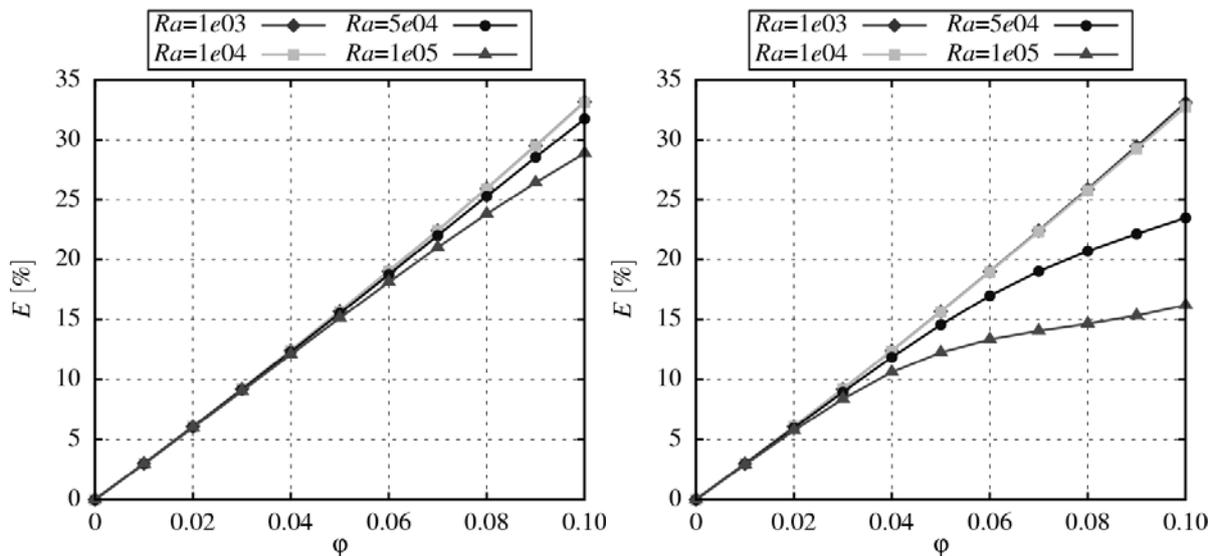

Figure 7: Heat transfer enhancement; Cu (left) and Au (right) water-based nanofluid.

5. CONCLUSIONS

Nanofluids play an important role in innovation processes from the perspective of organizations and widely to generate new value and to bring significant changes [18].

In the present study, the heat transfer characteristics of steady laminar natural convection water-based Au, Cu, Al_2O_3 and TiO_2 nanofluids in a square enclosure with differentially heated side walls have been studied by numerical means. The effects of Rayleigh number ($10^3 \leq Ra \leq 10^5$) and solid volume fraction ($0 \leq \varphi \leq 0,10$) have been systematically investigated.

The influence of computational grid refinement on the present numerical predictions was studied throughout the examination of grid convergence for natural convection of all types of water-based nanofluids at $Ra = 10^5$ and $\varphi = 0,10$. By utilizing extremely fine meshes the resulting discretisation error for the mean Nusselt number is well below 0,03 %.

Numerical method was validated for the case of natural convection of air ($Pr = 0,71$) in a square cavity for which the results are available in the open literature. Remarkable agreement of present results with the benchmark results yields sufficient confidence in present numerical procedure and results.

Highly accurate numerical results released some important points such as:

- Both increasing value of Rayleigh number and solid volume fraction of nanoparticles augment the heat transfer rate (mean Nusselt number).
- Mean Nusselt number $\overline{Nu}$ is an increasing function of both, Rayleigh number Ra and volume fraction φ of water-based nanofluids.
- Nanoparticles with the lowest value of thermal conductivity (TiO_2) are characterized with the lowest heat transfer in the conduction dominated heat transfer mode.
- Nanofluids with higher thermal diffusivity (Cu and especially Au) exhibit smaller relative increase of heat transfer in the convection dominated heat transfer mode.
- The effect of high conductive nanoparticles on heat transfer enhancement is more significant at low values of Rayleigh number (conduction dominated heat transfer).

6. ACKNOWLEDGEMENTS

REFERENCES

[1] Choi, S. U. S. (1995). Enhancing thermal conductivity of fluids with nanoparticles, Siginer, D. A.; Wang, H. P. (Eds.), *Developments Applications of Non-Newtonian Flows*, Vol. 66, 99-105, ASME, New York

[2] Micallef, D; Micallef, C. (2010). Mathematical model of a vapour absorption refrigeration unit, *International Journal of Simulation Modelling*, Vol. 9, No. 2, 86-97, doi:10.2507/ IJSIMM09(2)3.153

[3] Contuzzi, N.; Campanelli, S. L.; Ludovico, A. D. (2011). 3D finite element analysis in the selective laser melting process, *International Journal of Simulation Modelling*, Vol. 10, No. 3, 113-121, doi:10.2507/IJSIMM10(3)1.169

[4] Felde, I.; Reti, T. (2010). Evaluation Of Hardening Performance of Cooling Media by Using Inverse Heat Conduction Methods and Property Prediction, *Strojniski vestnik – Journal of Mechanical Engineering*, Vol. 56, No. 2, 77-83

[5] Oztop, H. F.; Abu-Nada, E. (2008). Numerical study of natural convection in partially heated rectangular enclosures filled with nanofluids, *International Journal of Heat and Fluid Flow*, Vol. 29, No. 5, 1326-1336, doi:10.1016/j.ijheatfluidflow.2008.04.009

[6] Hwang, K. S.; Lee, J.-H.; Jang, S. P. (2007). Buoyancy-driven heat transfer of water-based Al_2O_3 nanofluids in a rectangular cavity, *International Journal of Heat and Mass Transfer*, Vol. 50, No. 19-20, 4003-4010, doi:10.1016/j.ijheatmasstransfer.2007.01.037

[7]   Ho, C. J.; Chen, M. W.; Li, Z. W. (2008). Numerical simulation of natural convection of nanofluid in a square enclosure: effects due to uncertainties of viscosity and thermal conductivity, *International Journal of Heat and Mass Transfer*, Vol. 51, No. 17-18, 4506-4516, doi:10.1016/j.ijheatmasstransfer.2007.12.019

[8]   Saleh, H.; Roslan, R.; Hashim, I. (2011). Natural convection heat transfer in a nanofluid-filled trapezoidal enclosure, *International Journal of Heat and Mass Transfer*, Vol. 54, No. 1-3, 194-201, doi:10.1016/j.ijheatmasstransfer.2010.09.053

[9]   Oztop, H. F.; Abu-Nada, E.; Varol, Y.; Al-Salem, K. (2011). Computational analysis of non-isothermal temperature distribution on natural convection in nanofluid filled enclosures, *Superlattices and Microstructures*, Vol. 49, No. 4, 453-467, doi:10.1016/j.spmi.2011.01.002

[10] Abu-Nada, E.; Oztop, H. F. (2009). Effects of inclination angle on natural convection in enclosures filled with Cu-water nanofluid, *International Journal of Heat and Fluid Flow*, Vol. 30, No. 4, 669-678, doi:10.1016/j.ijheatfluidflow.2009.02.001

[11] Öğüt, E. B. (2009). Natural convection of water-based nanofluids in an inclined enclosure with a heat source, *International Journal of Thermal Sciences*, Vol. 48, No. 11, 2063-2073, doi:10.1016/j.ijthermalsci.2009.03.014

[12] Biluš, I.; Ternik, P.; Žunič, Z. (2011). Further contributions on the flow past a stationary and confined cylinder: Creeping and slowly moving flow of Power law fluids, *Journal of Fluids and Structures*, Vol. 27, No. 8, 1278-1295, doi:10.1016/j.jfluidstructs.2011.06.004

[13] Ternik, P. (2010). New contributions on laminar flow of inelastic non-Newtonian fluid in the two-dimensional symmetric expansion: Creeping and slowly moving conditions, *Journal of Non-Newtonian Fluid Mechanics*, Vol. 165, No. 19-20, 1400-1411, doi:10.1016/j.jnnfm.2010.07.007

[14] Roache, P. J. (1994). Perspective: A method for uniform reporting of grid refinement studies, *Journal of Fluids Engineering*, Vol. 116, No. 3, 405-413, doi:10.1115/1.2910291

[15] Ferziger, J. H.; Perić, M. (2002). *Computational Methods for Fluid Dynamics*, Springer-Verlag, Berlin

[16] De Vahl Davis, G. (1983). Natural convection of air in a square cavity: a bench mark numerical solution, *International Journal for Numerical Methods in Fluids*, Vol. 3, No. 3, 249-264, doi:10.1002/fld.1650030305

[17] Turan, O.; Chakraborty, N.; Poole, R. J. (2010). Laminar natural convection of Bingham fluids in a square enclosure with differentially heated side walls, *Journal of Non-Newtonian Fluid Mechanics*, Vol. 165, No. 15-16, 901-913, doi:10.1016/j.jnnfm.2010.04.013

[18] Palcic, I.; Buchmeister, B.; Polajnar, A. (2010). Analysis of Innovation Concepts in Slovenian Manufacturing Companies, *Strojniški vestnik – Journal of Mechanical Engineering*, Vol. 56, No. 12, 803-810